SQUID AXON MEMBRANE RESPONSE TO WHITE NOISE STIMULATION

RITA GUTTMAN, LANCE FELDMAN, *and* HAROLD LECAR

From the Department of Biology, Brooklyn College of the City University of New York, Brooklyn, New York 11210, and the Marine Biological Laboratory, Woods Hole, Massachusetts 02543, and the Laboratory of Biophysics, National Institute of Neurological Diseases and Stroke, National Institutes of Health, Bethesda, Maryland 20014

ABSTRACT The current from a white noise generator was applied as a stimulus to a space-clamped squid axon in double sucrose gap. The membrane current and the voltage response of the membrane were then amplified, recorded on magnetic tape, and the stimulus was cross-correlated with the response. With subthreshold stimuli, a cross-correlation function resembling that obtained from a resonant parallel circuit is obtained. As the intensity of the input noise is increased, the cross-correlation function resembles that obtained from a less damped oscillatory circuit. When the noise intensity is further increased so that an appreciable frequency of action potentials is observed, an additional component appears in the experimental cross-correlogram. The subthreshold cross-correlogram is analyzed theoretically in terms of the linearized Hodgkin-Huxley equations. The subthreshold axon approximates a parallel resonant circuit. The circuit parameters are temperature dependent, with resonant frequency varying from approximately 100 Hz at 10°C to approximately 250 Hz at 20°C. The Q_{10} of the resonant frequency is equal to 1.9. These values are in agreement with values found previously for subthreshold oscillations following a single action potential.

INTRODUCTION

Several physiological systems have been analyzed in terms of the response to white noise stimulation (Halpern and Alpert, 1971; Marmarelis and Naka, 1972; Stark, 1968). For linear systems, white noise analysis yields the response function of the system and can provide a convenient alternative to small signal AC analysis under certain circumstances. For nonlinear systems, the experimental white noise response has been used as the basis for a functional expansion description of the response of the system to general inputs (Wiener, 1958; George, 1959).

In the present study, we analyze the response of the space-clamped squid giant axon to white noise current stimulation. One of the motivations for this work is that the axon is a system whose response is accurately described by a set of differential equations (Hodgkin and Huxley, 1952), for which it is possible to compare the parameters obtained from white noise analysis with parameters predicted theoretically. In this way, one can build up a set of expectations with which to analyze the white noise

response of other nerve preparations for which an exact description based upon voltage clamp data may not exist.

Much of our study is confined to white noise in the subthreshold range of stimuli. This analysis is similar in spirit to the classic impedance studies of Cole and his collaborators (Cole, 1968) and to the sinusoidal small signal analysis of Mauro et al. (1970).

From the cross-correlation of stimulus and response, one can characterize the subthreshold membrane impedance in the linear region in terms of magnitude and phase. Thus, this method may provide a way to extend membrane impedance measurements to conditions where the AC bridge methods (Cole, 1968) are not convenient. The advantage of the use of white noise as a stimulus for a biological system is that one can measure the responses to all frequencies simultaneously. This is useful when studying biological systems which drift and have short lifetimes.

In addition to studying the linear region, we have investigated the effect of increasing the intensity of white noise stimuli from subthreshold to suprathreshold values. In the past, relatively simple wave forms, such as pulses, steps, linearly rising ramps, square waves, and sinusoids of current have been used as stimuli to investigate the excitability process in space-clamped squid axons (cf. Guttman, 1972; Guttman and Hachmeister, 1971). In the present study, the emphasis is less on a deterministic threshold criterion than on an analysis of the statistical correlates of random action-potential firing in response to noise as a stimulus. One application of this type of analysis is the prediction of axon firing in response to rapid and complex stimulation, as might occur when a nerve receives the convergence of many stimuli. This idea of white noise as a model for complex meaningful imputs has been exploited by Johanessma (1969).

MATERIALS AND METHODS

The method used in this study involved the application of various intensities of white noise (subthreshold, threshold, and suprathreshold) as stimuli to a space-clamped squid axon under double sucrose gap. The method of mounting the axon in the chamber, the stimulating and recording circuit, and the analysis circuit are illustrated in Fig. 1.

The axon was mounted in a chamber internally divided into five compartments, A, B, C, D, and E. The extreme compartments, A and E, were filled with 500 mM KCl, which served to inactivate those portions. Compartments B and D contained flowing isosmotic sucrose (0.75 M). Compartment C, the experimental compartment, contained flowing artificial sea water.

The current from a noise generator (HP-8057A, Hewlett-Packard, Co., Palo Alto, Calif.) was applied as a stimulus to platinized platinum electrodes situated in compartment A and C. Stimulation consisted of 15-s applications of noise current of constant intensity over a bandwidth 7 Hz to 10 KHz. The potential response was picked up by a silver-silver chloride electrode in compartments C and E.

The portion of the axon in the central compartment was close to the current electrode, which filled the entire length of that compartment. An approximately uniform current density in the neighborhood of the electrode was expected because the length of the axon between the

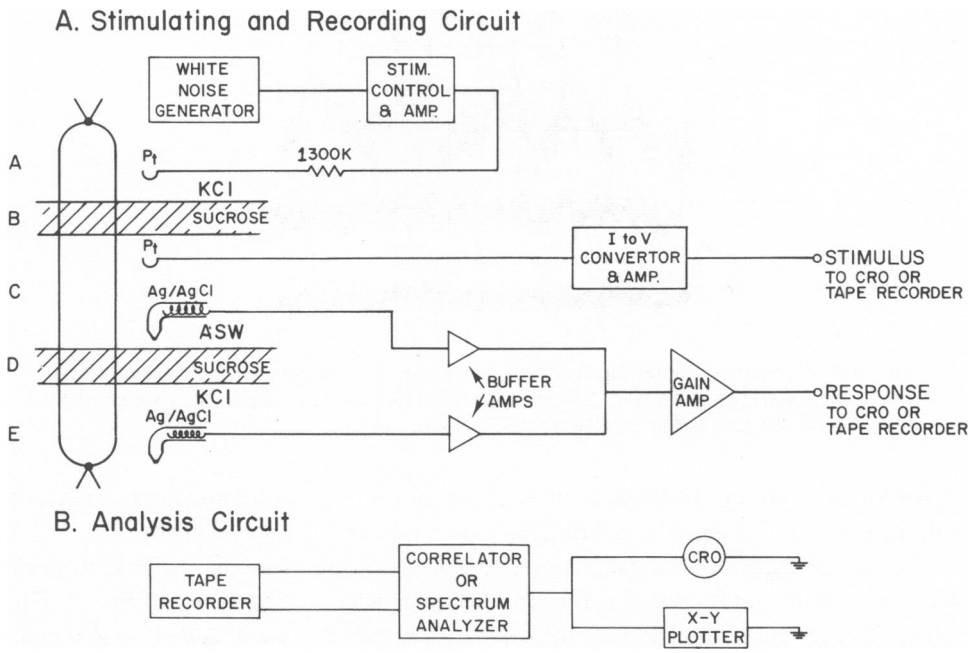

FIGURE 1 A, stimulating and recording circuit and B, analysis circuit for study of space-clamped squid axon membrane response to white noise stimulation by means of cross-correlation technique. Double sucrose gap utilized for space-clamping. See text for details.

sucrose compartments was 0.8 mm, considerably less than the "characteristic length" of approximately 6 mm found for squid axon at rest (Cole and Hodgkin, 1939).

The membrane current and the voltage response of the membrane were then amplified and recorded on magnetic tape for later analysis, or analyzed on line. The stimulus was cross-correlated with the response with appropriate scaling on a Saicor 43A correlator (Honeywell Test Instrument Division, Hauppauge, N.Y.). The correlator is an on-line special purpose digital computer which computes the time average of the product of one signal with a time-delayed version of a second signal. The cross-correlograms (CCG) measured in our experiments are the time average of the product of stimulating current and membrane potential taken as a function of a variable time delay. The cross-correlation functions were recorded on an X-Y plotter.

EXPERIMENTAL RESULTS

A sequence of typical voltage responses to varying intensity of white noise stimulation is shown in Fig. 2. In the bottom record (4.24 μA root mean square [rms] stimulus) the response appears to be a typical bandwidth limited noise record with no evidence of excitation. The middle record (7.46 μA stimulus) shows increased noise and an occasional action potential, corresponding to a mean rate of firing of the order of 10 per second. The top trace shows the response to a high intensity stimulus (13.3 μA). In this record the firing rate is approximately 100 per second. The three regimes illus-

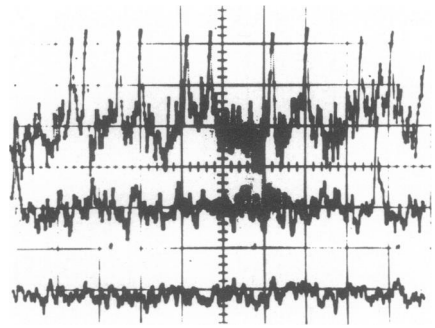

FIGURE 2 Cathode ray oscilloscope displays of responses of space-clamped squid axon to white noise, subthreshold (4.24 μA rms), bottom; threshold (7.46 μA rms), middle; and suprathreshold (13.3 μA rms), top. Calibration, 50 mV/div; 10 ms/div; 15°C.

trated by the figure can be thought of as subthreshold, threshold, and suprathreshold, although any precise definition of threshold for a random stimulus is arbitrary.

The most straightforward characterization of the output noise in response to input white noise is the output power spectrum. A typical spectrum is shown in Fig. 3. The salient features of the spectrum are the resonance centered at about 260 Hz, and a high-frequency falloff consistent with an underdamped second-order response. As the input noise intensity is increased the output noise not only increases but exhibits increasing resonant character, as if increased noise intensity introduces negative damping with only a small change in the resonant frequency of the system.

The most useful quantity for systems analysis is the cross-correlogram (CCG) between the input white noise and the output noise. Fig. 4 shows CCGs taken with varying input noise intensity. Again we see an increase in resonant character of the

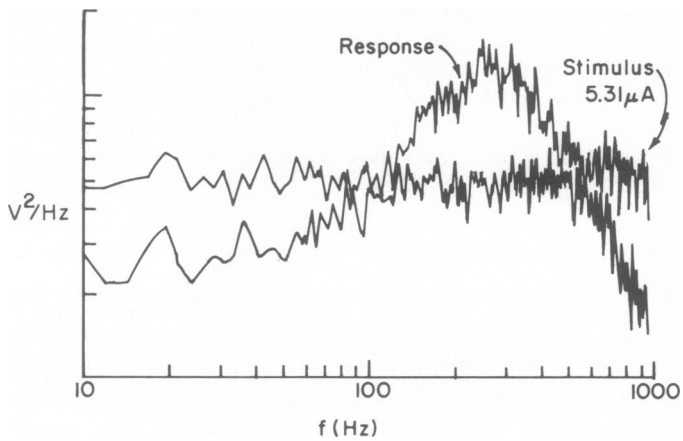

FIGURE 3 Spectrum analysis of voltage response of squid axon membrane to threshold white noise current stimulus. Frequency in hertz vs. power density in volts^2 per hertz in arbitrary units. Note resonant frequency of response is approximately 260 Hz. Temperature 15°C.

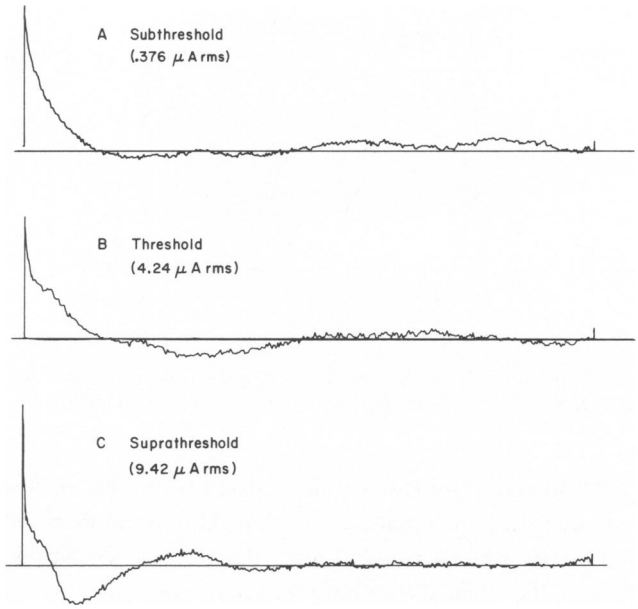

FIGURE 4 *a* Cross correlogram of input current noise and output voltage response measured for three values of stimulating current. A, subthreshold stimulus, 0.376 μA rms; B, threshold stimulus, 4.24 μA rms; C, suprathreshold stimulus, 9.42 μA rms. These three cross-correlograms correspond to the three types of output record shown in Fig. 2. Total elapsed time represented on *x* axis is 20 ms.

response as the stimulus intensity is increased. The response resembles that expected for a parallel RLC circuit, but with progressively less damping. One new feature which appears when stimulus intensity is further increased is a plateau whose appearance coincides with the threshold; the suprathreshold CCG appears to contain two components—a component expected from a parallel RLC circuit and a component correlated to the onset of action potentials (Fig. 4 *b*).

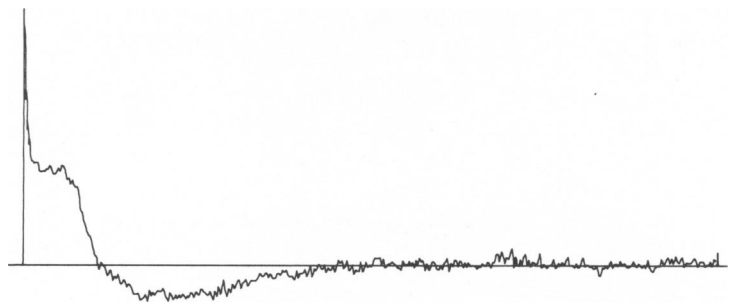

FIGURE 4 *b* Correlogram of suprathreshold white noise stimulus and response of squid axon membrane showing damped sinusoidal oscillations characteristic of a resonant circuit, and additional "plateau" component characteristic of random spike train output. Total time, 10 ms.

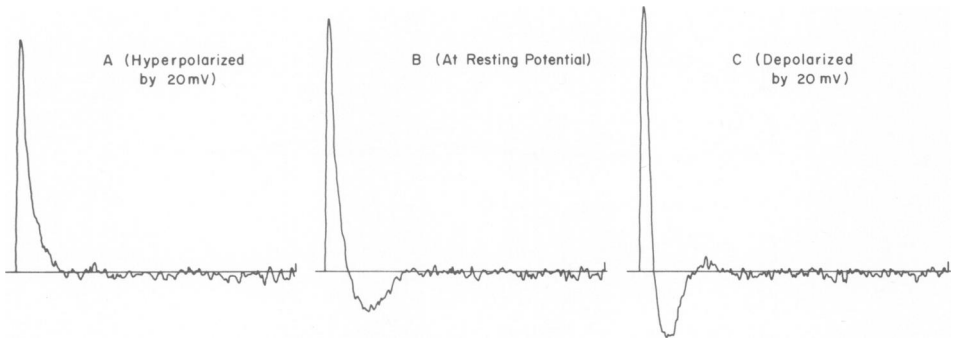

FIGURE 5 Correlation functions of white noise stimulus and voltage response for an axon: A, hyperpolarized by 20 mV; B, at the resting potential and C, depolarized by 20 mV. x and y axes as in Fig. 4.

It should be mentioned that some variability existed from fiber to fiber in the degree of damping at any one stimulus intensity and that there were fibers with good resting potential and excitability which exhibited more damping at threshold than shown in Fig. 4. However, as the fiber died, the amount of damping invariably increased, whatever it was initially.

There seem to be no simple indices or general agreement as to the "condition" of an experimental axon. In two attempts FitzHugh (1966) has introduced such a parameter and Fishman (personal communication) has followed axon deterioration in voltage clamp under conditions of internal perfusion. The most common requirement for good axons are probably resting and action potentials of 60 mV and 100 mV and a threshold of 15 mV.

Changes in the CCG can also be demonstrated for the subthreshold range of stimuli by introducing a constant current superimposed on the noise current. The constant current places a depolarizing or hyperpolarizing bias on the axon and effectively changes the operating point. This is illustrated in Fig. 5. For small noise intensity,

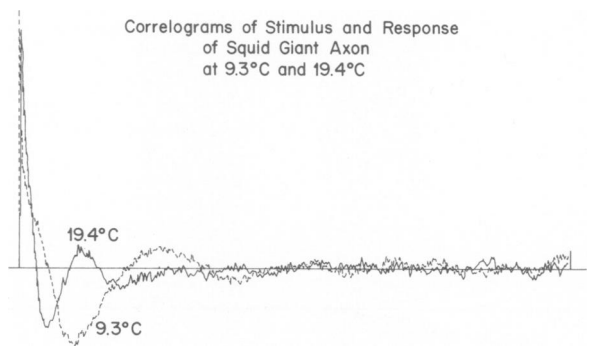

FIGURE 6 *a* Superimposed CCGs of white noise stimulus and space-clamped squid axon response for the two temperatures: 9.3°C and 19.4°C. The approximately 10°C increase in temperature results in an increase in frequency of oscillation. x and y axes as in Fig. 4 *a*.

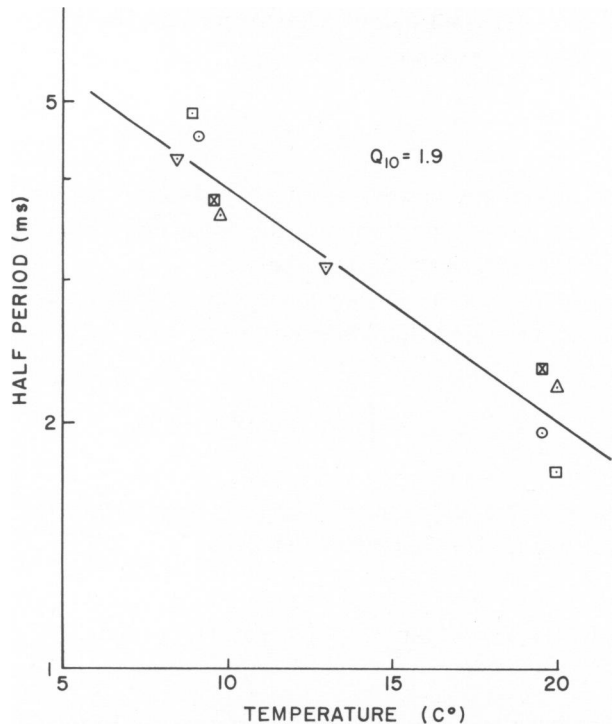

FIGURE 6 *b* Effect of temperature on rate of oscillation in CCG of random white noise stimulus input and squid membrane response. Temperature in degrees centigrade vs. half-period in milliseconds. Slope indicates a Q_{10} of 1.9. Half-period was measured between first minimum and subsequent maximum of the CCG. Intercepts of the individual semilog plots were adjusted in order to display a single best-fit line.

one might expect such measurements to provide the small signal impedance characteristic of the axon, about a particular operating point. The analysis in terms of the linearized Hodgkin-Huxley equations is discussed in the next section, and one result of the analysis is the computation of linear CCGs for different operating points as illustrated in Fig. 9.

The results of a preliminary study of the effect of temperature upon the cross-correlation function are demonstrated in Fig. 6. In Fig. 6 *a*, CCGs of an axon at two different temperatures, 9.3°C and 19.4°C, approximately 10°C apart, are shown. In this figure the frequency of oscillation of the CCG increased markedly with temperature increase. When temperature is plotted against half-period of oscillation for five axons (Fig. 6 *b*), the slope of the curve obtained gives a Q_{10} of 1.9.

ANALYSIS AND DISCUSSION

Linear Region

The response of the axon to low level noise inputs can be accounted for entirely in terms of the linearized Hodgkin-Huxley equations. For a linear system, it can be

shown (Lee, 1960) that the input-output relations between the power spectra of input current noise and output voltage noise is given by

$$\Phi_v(\omega) = |\mathcal{Z}(\omega)|^2 \Phi_I(\omega), \tag{1}$$

where $\mathcal{Z}(\omega)$ is the membrane impedance. For white-noise current, $\Phi_I(\omega)$ is a constant, and the voltage power spectrum has the same frequency dependence as the square absolute value of the membrane impedance.

It can also be shown that the cross-correlogram is the convolution of the unit impulse response and the input autocorrelation. Thus,

$$\varphi_{io}(\tau) = \int_{-\infty}^{\infty} h(v)\, \varphi_{ii}(\tau - v)\, dv, \tag{2}$$

where τ is correlation time, $h(\nu)$ is the unit impulse response for the membrane, and the autocorrelation of a random function is defined by

$$\varphi_{ii}(\tau) = \lim_{T \to \infty} \frac{1}{2T} \int_{-T}^{T} f(t) f(t + \tau)\, dt. \tag{3}$$

For a white noise input the autocorrelation is proportional to the unit impulse (since idealized random noise should show no correlations for time intervals greater than zero). Thus,

$$\varphi_{ii}(\tau) = 2\pi K u(\tau), \tag{4}$$

where K is a constant with dimension of V^2 and $u(\tau)$ is the unit impulse. Substituting Eq. 4 into Eq. 2 leads to the relation

$$\varphi_{io}(\tau) = 2\pi K h(\tau), \tag{5}$$

showing that the cross-correlation has the form of the impulse response of the membrane impedance. It is often useful to recall that the impulse response function can be written as the Fourier transform of the membrane impedance.

The impedance properties of the axon membrane have been studied extensively by Cole (1968). The admittance of the linearized Hodgkin-Huxley axon can be written in the form similar to that employed by Chandler et al. (1962):

$$Y(\omega) = g_\infty + j\omega c_m + \sum_{i=1}^{3} g_i/(1 + j\omega\tau_i), \tag{6}$$

where the g_i can be defined in terms of voltage-dependent rates appearing in the

Hodgkin-Huxley equations; i.e.,

$$\begin{aligned} g_1 \equiv g_m &= 3m_\infty^2 h_\infty \tau_m \bar{g}_{Na}(V - V_{Na})[\alpha_m' - (\alpha_m' + \beta_m')m_\infty] \\ g_2 \equiv g_n &= 4n_\infty^3 \tau_n \bar{g}_K(V - V_K)[\alpha_n' - (\alpha_n' + \beta_n')n_\infty] \\ g_3 \equiv g_h &= m_\infty^3 \tau_h \bar{g}_{Na}(V - V_{Na})[\alpha_h' - (\alpha_h' + \beta_h')h_\infty] \\ g_\infty &= \bar{g}_{Na} m_\infty^3 h_\infty + \bar{g}_K n_\infty^4 + \bar{g}_L. \end{aligned} \tag{7}$$

All of the parameters in Eq. 8 have their usual definitions (Chandler et al., 1962). The impedance of the membrane is, of course, given by the reciprocal of the admittance.

The impedance can be written as

$$\mathcal{Z}(p) = \frac{Ap^3 + Bp^2 + Cp + 1}{Ep^4 + Fp^3 + Gp^2 + Hp + I}, \tag{8}$$

where

$$\begin{aligned} p &= j\omega \\ A &= \tau_m \tau_n \tau_h \\ B &= \tau_m \tau_n + \tau_m \tau_h + \tau_n \tau_h \\ C &= \tau_m + \tau_n + \tau_h \\ E &= AC_m \\ F &= Ag_\infty + BC_m \\ G &= Bg_\infty + CC_m + g_m \tau_n \tau_h + g_n \tau_m \tau_h + g_h \tau_m \tau_n \\ H &= Cg_\infty + C_m + g_m(\tau_n + \tau_h) + g_n(\tau_m + \tau_h) + g_h(\tau_m + \tau_n) \\ I &= g_\infty + g_m + g_h \end{aligned} \tag{9}$$

It is convenient to present computations employing the standard values of the Hodgkin-Huxley parameters (FitzHugh, 1969). These standard values are: $g_1 = -0.4315$ mmho/cm^2, $g_2 = 0.8489$ mmho/cm^2, $g_3 = 0.0716$ mmho/cm^2, $g_\infty = 0.678$ mmho/cm^2, $\tau_m = 0.2368$ ms, $\tau_n = 5.4586$ ms, $\tau_h = 8.516$ ms, $c = 1$ μF/cm^2, $T = 6.3$°C. The various voltage-dependent functions, such as α_m, β_m, etc. can be taken from the original work of Hodgkin and Huxley (1952) or from standard references such as Cole (1968) or FitzHugh (1969). The main variable parameters for describing the present experiments are the leakage conductance, g_L, which varies from preparation to preparation, and the temperature. By varying leakage values and correcting for the known temperature dependance of the Hodgkin-Huxley rates (FitzHugh, 1969), we were able to fit the subthreshold experimental results of Figs. 3–6. However, in the following discussion, we emphasize results computed for the standard

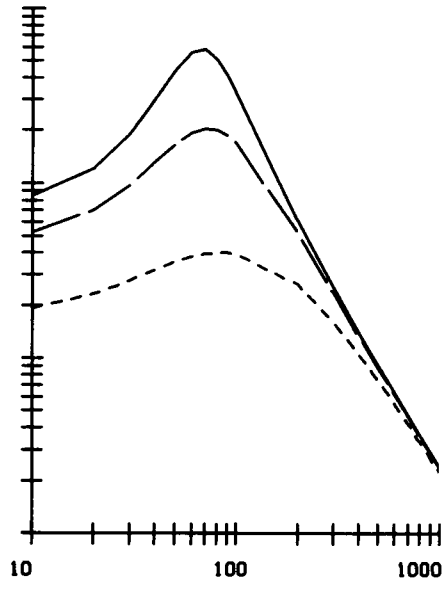

FIGURE 7

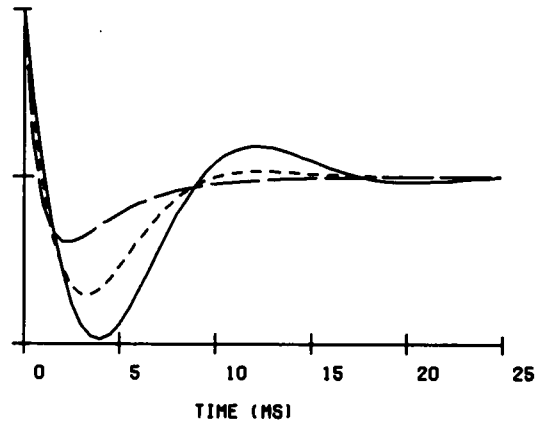

FIGURE 8

FIGURE 7 Power spectrum calculated from the linearized Hodgkin-Huxley equations. The solid curve shows standard conditions, temperature 6.3°C, leakage 0.3 mmho/cm^2. The dashed curves show effect of increased leakage to twice and five times nominal value.

FIGURE 8 Cross-correlogram calculated from linearized Hodgkin-Huxley equations. Solid curve shows CCG for 0.3 mmho/cm^2 leakage and dashed curves show effects of increased leakage as in Fig. 7.

conditions of leakage and temperature because these conditions coincide with most other analyses in the literature.

Fig. 7 shows the voltage power spectrum computed from the absolute value of the impedance squared of Eq. 9 using the definition of Eq. 1. Fig. 8 shows the CCG computed from the linearized Hodgkin-Huxley equations. In both figures, the varying values of leakage were inserted to show the range of response expected for the actual preparation, which is considerably more leaky than the theoretical axon. The power spectrum and CCG were calculated for temperature equal to 6.3°C, the normal temperatures for the Hodgkin-Huxley parameters.

Fig. 9 shows the variation of the CCG with depolarization and hyperpolarization of 10 mV as computed from the linearized Hodgkin-Huxley equations.

The values of the parameters computed for these conditions are: for 10 mV hyperpolarization, $g_l = -0.0182$ mmho/cm^2, $g_2 = 0.0198$ mmho/cm^2, $g_3 = 0.0009$ mmho/cm^2, $\tau_m = 0.1412$ ms, $\tau_n = 5.7821$ ms, $\tau_h = 7.4964$ ms; for 10 mV depolarization, $g_l = -0.3881$ mmho/cm^2, $g_2 = 5.3084$ mmho/cm^2, $g_3 = 1.3303$ mmho/cm^2, $\tau_m = 0.3669$ ms, $\tau_n = 4.7548$ ms, $\tau_h = 6.1858$ ms. This variation is qualitatively

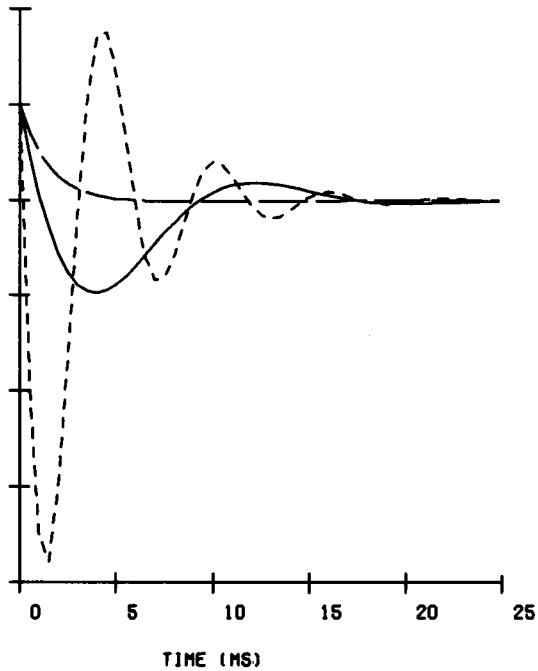

FIGURE 9 Cross-correlogram calculated from linearized Hodgkin-Huxley equations, showing effect of hyperpolarization and depolarization. Theoretical figure is comparable to data of Fig. 5.

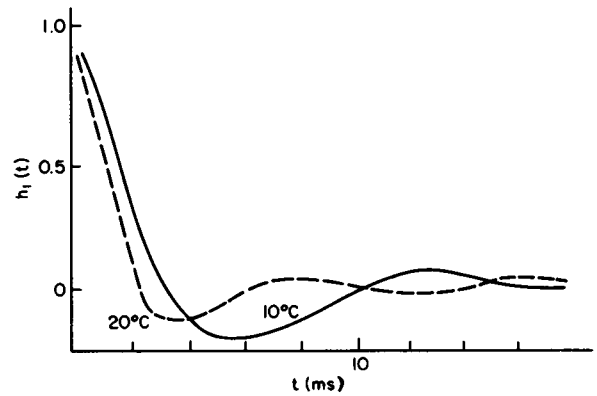

FIGURE 10 Effect of temperature on CCG as calculated from linearized Hodgkin-Huxley equations. Theoretical variation of resonant frequency with temperature is comparable to experimental variation shown in Fig. 6 *a*.

consistent with the experimental data shown in Fig. 6, although quantitative agreement depends on the value of leakage conductance chosen. We note that the data reported here on the resonant frequency of the CCG is in agreement with earlier data on the subthreshold oscillations which follow an action potential spike (Guttman, 1969).

RELATION TO SIMPLE IMPEDANCE FUNCTIONS

Subthreshold impedance measurements are generally analyzed in terms of simpler lumped parameter circuits than the fourth-order linearized Hodgkin-Huxley network (Cole, 1968). One instructive way of relating the exact circuit to a simple RLC network is to note the following approximations which prevail near the resting state.

Let us assume that the sodium activation process, which is much faster than the other two processes, occurs instantaneously ($\tau_m \approx 0$). This approximation should be valid for frequencies below $\approx$1,000 Hz. Further, the parameter g_h, in Eq. 7 is much smaller than g_n or g_m, so we can ignore g_h near rest.

With these approximations, Eq. 6 reduces to the admittance of a parallel resonant network,

$$Y_0(p) = g_\infty + g_m + C_m p + g_n/(1 + p\tau n). \tag{10}$$

Here sodium has its entire effect as an instantaneously responding negative resistance, and the inductance comes entirely from the linearized potassium process. Taking the reciprocal of Eq. 10, we arrive at an impedance function,

$$Z_0(p) = \frac{1 + p\tau_n}{g^* + C^* p + C_m \tau_n p^2}, \tag{11}$$

where

$$g^* = g_\infty + g_m + g_n, \tag{11A}$$

$$C^* = C_m + (g_\infty + g_m)\tau_n. \tag{11B}$$

It is convenient to define a resonance frequency parameter,

$$\omega_0 = (g^*/C_m \tau_n)^{1/2}, \tag{12}$$

and a damping time constant

$$T_0 = 2C^*/g^*. \tag{12A}$$

We note that Eq. 11 is not the most general expression that can be written, because the approximations employed are valid only when the finite time delay of the Na process is not evident in the frequency response. We refer the reader to the book by Cole (1968) for an analysis in terms of a more general biquadratic expression.

Eq. 11 does however give a good approximation for calculating the power spectrum and cross-correlogram as will be shown next. From Eq. 11, the power spectrum can be written as

$$\Phi_V(\omega) = \Phi_V(0)\frac{1 + \omega^2\tau_n^2}{[(1 - (\omega/\omega_0)^2]^2 + (\omega T_0/2)^2}. \tag{13}$$

The impulse response leading to the cross correlation function is obtained by solving the circuit differential equation or by taking the inverse transform of Eq. 11. The expression is

$$h(t) = e^{-t/T_0}[\cos(\omega^* t) - (T_0\omega^*)^{-1}\sin(\omega^* t)],$$

where

$$\omega^* = \omega_0(1 - (\omega_0 T_0)^{-2})^{1/2}. \tag{15}$$

We note that the term $\omega_0 T_0$ appearing in Eq. 15 is a measure of the sharpness of the resonance appearing in the spectra of Fig. 7. Consequently, from the shape of the spectrum, we can estimate g^* and, through g^*, the leakage conductance for a particular preparation.

The neglected terms do not affect the results much near rest. The analytic expressions have the virtue that they can be fit to the data and the parameters determined. Furthermore, Eqs. 12 and 15 give the resonant frequency and damping factor of the network in terms of Hodgkin-Huxley parameters.

As an application of Eqs. 11–15, we can estimate the resonance frequency and damping time constant for various experimental conditions. For the standard conditions of the Hodgkin-Huxley parameters, $g_L = 0.3$ mmho/cm^2 and $T = 6.3$°C, the values computed from Eqs. 11, 12, and 15 are: $f_{res} = \omega^*/2\pi = 69$ Hz, and $T_0 = 4.27$ ms. For the sucrose gap preparation, at 22°C, we can assume that the main temperature dependence is through the factor τ_n, for which we know the Q_{10} is 3. If we guess that g_L is five times the nominal standard value, Eqs. 11, 12, and 15 give $f_{res} = 232$ Hz and $T_0 = 2.09$ ms. For leakage value 10 times the standard value, the equations give $f_{res} = 307$ Hz, $T_0 = 2.04$ ms. Typical experimental values are $f_{res} = 296$ Hz and $T_0 = 1.27$ ms. Thus the simplified equations seem most consistent with the higher leakage value. More important than the exact quantitative fit is the fact that Eq. 12 gives a qualitative account of the temperature dependence of Fig. 6 *b*.

NONLINEAR EFFECTS

As the noise intensity is increased, two different types of nonlinearity can be seen in the CCGs. For noise intensities in the threshold range the CCGs still have the shape of the linear CCG, but the damping decreases with increasing noise intensity. This continuous change in a circuit parameter can be termed mild nonlinearity. As the

noise intensity is further increased into the suprathreshold range, a second type of nonlinearity, the "plateau" component appears in the CCG. Mild nonlinearity is evident in Fig. 4 *a* and "plateau" nonlinearity is illustrated in Fig. 4 *b*.

The mild nonlinear behavior might be expected from the rectification of the input noise by the voltage-dependent conductance parameters. A rectification leading to an average depolarization would reduce the damping as shown in Fig. 4 *a*. We have performed one computation which illustrates this behavior. By analogy to the theorem for linear systems relating the CCG to the impulse response, we computed the subthreshold impulse response for the exact (not linearized) Hodgkin-Huxley equations. As the magnitude of the initial impulse was increased in these computations, the impulse response functions showed decreased damping and more or less constant frequency similar to the experimental CCGs.

The second type of nonlinearity, the "plateau" component of the CCG appears to be correlated to the onset of action-potential firing. As noise intensity is increased in the suprathreshold domain the plateau increases in amplitude along with the rate of firing, and both the plateau and the firing rate appear to saturate at very high noise intensities.

An analysis of the action-potential component has been presented (Lecar, 1973) which gives a qualitative account of these features. The plateau component of the CCG was calculated by assuming that a Poisson sequence of action potentials is keyed to a random sequence of suprathreshold input noise peaks. In order to obtain agreement with experiment two features of action-potential firing had to be considered—the threshold criterion, and the variable latency of firing. For bandwidth limited white noise stimulation (filtered by the linearized membrane impedance) one can assume the Hodgkin-Huxley axon obeys a constant charge threshold law. For such a law, the distribution of stimuli in excess of threshold by some amount of charge was estimated using the theory of noisy relays (Stratanovich, 1963). For any particular suprathreshold stimulus value an associated latency value could be estimated either from experimental latency distribution curves (Ten Hoopen and Verveen, 1959) or from a theoretical expression (Lecar and Nossal, 1971). When the "threshold-excess" and latency distribution functions are convoluted with the action-potential shape function a CCG shape in agreement with the plateau term is obtained. The amplitude of this plateau does indeed saturate with increasing noise intensity.

It thus appears possible to analyze some of the nonlinear behavior seen in the CCG, but a complete analysis would require more thorough study of the changes in CCG and the frequency of firing as noise intensity is increased. In particular for very high noise intensities the train of action potentials stimulated by noise will depart from a Poisson process as the average interval between action potentials approaches the duration of the refractory period. It would be of interest to observe how this onset of periodicity is reflected in the CCG.

The authors would like to thank Doctors K. S. Cole and H. Fishman for their valuable discussions of this work.

The work has been aided by National Science Foundation grants GB-28527 and GB-38355 awarded to one of us (R. Guttman).

Received for publication 8 July 1974 and in revised form 1 October 1974.

REFERENCES

CHANDLER, W. K., R. FITZHUGH, and K. S. COLE. 1962. *Biophys. J.* **2**:105.

COLE, K. S., and A. L. HODGKIN. 1939. *J. Gen. Physiol.* **25**:29.

COLE, K. S. 1968. Membranes, Ions and Impulses. University of California Press, Berkeley.

COLE, K. S., and A. L. HODGKIN. 1939. *J. Gen. Physiol.* **22**:671.

FITZHUGH, R. 1966. *J. Gen. Physiol.* **49**:989.

FITZHUGH, R. 1969. *In* Biological Engineering. H. P. Schwan, editor. McGraw-Hill Book Co., Inc., New York. 1–85.

GEORGE, D. A. 1959. Technical Report 355. Research Laboratory of Electronics, Massachusetts Institute of Technology, Cambridge.

GUTTMAN, R. 1969. *Biophys. J.* **9**:269.

GUTTMAN, R. 1972. *In* Perspectives in Membrane Biophysics. D. P. Agin, editor. Gordon and Breach, New York. 147.

GUTTMAN, R., and L. HACHMEISTER. 1971. *J. Gen. Physiol.* **58**:304.

HALPERN, W., and N. R. ALPERT. 1971. *J. Appl. Physiol.* **31**:913.

HODGKIN, A. L., and A. F. HUXLEY. 1952. *J. Physiol.* **116**:500.

JOHANESSMA, P. I. M. 1969. Dissertation. Catholic University of Nijmegen, Holland.

LECAR, H. 1973. *Biophys. Soc. Abstr.* **13**:168*a*.

LECAR, H., and NOSSAL, R. 1971. *Biophys. J.* **11**:1048.

LEE, Y. W. 1960. Statistical Communication Theory. John Wiley and Sons, Inc., New York.

MARMARELIS, P. Z., and K. NAKA. 1972. *Science (Wash. D.C.).* **175**:1276.

MAURO, A., F. CONTI, F. DODGE, and R. SCHOR. 1970. *J. Gen. Physiol.* **55**:497.

RICE, S. O. 1954. Mathematical analysis of random noise. (*Bell Syst. Tech. J.*, vols. 23, 24). *Reprinted in* Noise and Stochastic Processes. N. Wax, editor. Dover Publications, Inc., New York.

STARK, L. 1968. Neurological Control Systems. Plenum Press, New York.

STRATANOVICH, R. L. 1963. Topics in the Theory of Random Noise. Vol. II. Gordon and Breach, New York.

TEN HOOPEN, M., and A. A. VERVEEN. 1963. *Proceedings of the International Conference on Cybernetics in Medicine.* N. Wiener and J. P. Schade, editors. Elsevier Publishing Co., Amsterdam.

WIENER, N. 1958. Nonlinear Problems in Random Theory. Massachusetts Institute of Technology Press, Cambridge.